



Article Processing Dates: Received on 2022-09-04, Reviewed on 2022-10-11, Revised on 2022-10-23, Accepted on 2022-10-27, and Available online on 2023-04-25

The effect of variations in electric load on the performance of a 3 kW Micro Hydro Power Plant using an undershot waterwheel

Yusuf Dewantoro Herlambang^{1*}, Bono¹, Gatot Suwoto¹, Suwarti¹, Baktiyar Mei Hermawan¹, F Gatot Sumarno¹, Margana¹, Marliyati³

¹Department of Mechanical Engineering, Politeknik Negeri Semarang, Semarang 50275, Indonesia

²Department of Accounting, Politeknik Negeri Semarang, Semarang 50275, Indonesia

*Corresponding author: masyusufdh@polines.ac.id

Abstract

The purpose of this study is to evaluate the performance of the undershot water wheel type with a 3 kW generator as a micro-hydro power plant that generates electricity by utilizing water power from paddy fields and local resources. Where the irrigation canal can irrigate approximately 247 hectares of rice fields during the dry season. The research technique employs a waterwheel with a 1.1-meter diameter, 12 blades with a 70-centimeter blade arm length, and a 2-inch shaft diameter. The transmission system employs a chain to increase rotation and decrease slippage and rotation losses, making it simpler to drive the generator to produce electricity. The test was conducted by varying the lamp capacity from 100 W to 800 W while maintaining constant water discharge and flow. Water discharge, water head, generator rotation, electric current traveling through the load, and output voltage are the test parameters. With a discharge of 0.476 m³/s, a water flow speed of 3.229 m/s, a waterwheel rotation of 42.39 rpm, and electric power of 207 W, the utmost efficiency value of 8.35% was determined.

Keywords: Undershot waterwheel, electric load, generator power, waterwheel rotation, efficiency

1 Introduction

In tandem with the depletion of fossil fuels, the annual growth rate of Indonesia's electrical energy consumption is constant. This impacts Indonesia's elevated electricity demand [1-5]. According to data from the Indonesian Consumers Foundation (YLKI), approximately 40 million Indonesians have not had access to electricity for a complete day, representing approximately 20% of the population. A total of 2,519 villages (mostly in four provinces: Papua, Maluku, Central Kalimantan, and Maluku) have not received electricity from PLN, and there are still approximately 12,659 villages out of a total of 82,190 villages in Indonesia without electricity. Therefore, efforts are being made to satisfy the demand for electrical energy by utilizing micro-hydro power plants. Micro-hydro is a small-scale hydroelectric power facility with a per-unit capacity limit of 5 kW to 1 MW. Utilizing the energy of the watershed is one method of using micro-hydro power facilities (DAS).

A river flow suitable for use as a source of driving energy for micro hydro is one that flows year-round and has a consistent

discharge throughout the seasons. In reality, not all river flow rates are constant, and many watersheds have relatively modest discharges.

Utilization of the kinetic energy of river flow with several already-known waterwheels, such as the container model waterwheel, overshot, undershot, and undershot [6-8]. The technology of small-scale micro-hydro power facilities using several waterwheels above has been patented, including Japanese patent no. JP2013127234A relates to waterwheels with variable blade angles in the overshot (overshot) water flow. US patent no. US2019/0186457A1 has patented an undershot type waterwheel that increases its wheel's power by directing a civil dam structure toward its torso. European patent no. WO/2017/220995A1 has also obtained a patent on the undershot type waterwheel by configuring the blades to enhance the inflow energy to the waterwheel's blades. With respect to the majority of existing patents, no combination of civil structures with undershot waterwheels for power generation in open flow [9-10] at varying discharge and electrical load flows (for irrigation canals and rivers in rural areas) with complete specifications have yet been accomplished.

In addition to the gravitational potential energy, the influence of the weight of the water flowing into the blades must be regarded in the waterwheel [11-13]. The acceptable water drop height for the wheel is between 0.1 m and 12 m, and the water capacity is between 0.05 m³/s and 5 m³/s. The waterwheel is utilized in regions where the water discharge is variable and the water level is low. A waterwheel [14-16] with a slow rotation speed can be made of wood, whereas a waterwheel with a high rotation speed and enormous waterfalls can be made of iron.

The waterwheel is a device that converts the kinetic energy of water into mechanical energy [17-20], with the thrust of the water flow causing the axis of the wheel to rotate. This rotating wheel drives an electrical generator. Thus, electricity will be produced that can be utilized for a variety of purposes. The flowing water will strike the wheel's blades, causing the wheel to receive a number of forces that cause it to move. The operation of the waterwheel generates electricity until multiple energy transformations occur due to electricity consumption. The same principle applies to the use of electrical energy in this study as it does to other renewable energy generators, such as solar cells and fuel cells [21-22].

The first is the transformation of water's potential energy into mechanical energy (motion) by the wheel. Both of these mechanical energies will rotate the generator, causing electrons to leap due to the generator's rotation. This results in an electromagnetic current. The electric current is then distributed to residences, rooms, factories, and anything else that requires it. Here, depending on the need, the electric current is converted into light energy for lamps or illumination, as in iron or oven, or into fan propulsion, machines, and the like [23-25].

Utilizing the height of the descending water and the water capacity, waterwheels are the most commonly imitated method of its production. In addition to the gravitational potential energy, the influence of the weight of the water flowing into the blades must be regarded in the waterwheel [26-28]. The acceptable water drop height for the wheel is between 0.1 m and 12 m, and the water capacity is between 0.05 m³/s and 5 m³/s. The waterwheel is utilized in regions where the water discharge is variable and the water level is low. If the rotational speed is low and the cascades are large, the material for the waterwheel can be wood, but if the rotational speed is high and the waterfalls are large, the waterwheel can be made of iron [22].

Consequently, developing a model of an undershot type combination waterwheel with a blade curvature angle of 30 degrees to the flow of water discharge and electrical loading variations is necessary for optimal performance. The waterwheel

can serve as the driving force for a Microhydro Power Plant (MHP). The application of this undershot waterwheel with a robust and sturdy galvalume plate blade as the prime mover for other loads such as electricity generators is still uncommon or nonexistent, particularly in Indonesia, which has low water flow rates, particularly around irrigation waterways or river flows. Therefore, this research represents an innovation in the application of undershot waterwheels to open-channel systems as micro hydropower facilities [29-31]. Examine the experimental model of the combination breastshot and overshot waterwheel with a 30-degree blade curvature angle.

2 Materials and Procedures

2.1 Materials

The stages of this research are conducted beginning with the process of manufacturing waterwheels based on previously determined design drawings, planning proportions, and calculations. In the second stage of manufacturing the Waterwheel blades, the type of material to be used is determined; specifically, 4 used drums with a thickness of 1.5 mm divided into 3 parts with a height of 700 mm to produce some blades of the wheel and a 2-mm-thick iron plate to cover the waterwheel. The diameter of the waterwheel is 1100 mm, and its 12 blades are 700 mm wide. The shaft is composed of AISI 1045 solid shaft steel with a diameter of 50.8 mm and a length of 1300 mm.

The manufacturing apparatus for the waterwheel consists of a lathe and its accessories, an electric welding machine and its accessories, a drilling machine, a cutting grinding machine, a hacksaw, a steel ruler, a ring wrench, a plate cutter, a screwdriver, an L wrench, and one set of tapping. The third step involves varying the lamp capacity from 100 W to 800 W to test the waterwheel on an open channel for agricultural irrigation. The next step is to examine the characteristics of the waterwheel based on the results of the experiments conducted in order to achieve optimal performance according to the waterwheel's specifications.

The test measures the head on the flow channel, the rotation of the generator shaft as measured by a manual tachometer, the speed of the water flow as measured by a flow watch, and the voltage and current of the generator as measured by the measuring instrument. While these data are used to calculate the discharge, hydraulic power, electrical power, and efficiency of the turbine. All data is presented in tabular format with illustrative graphs in order to facilitate discussion and analysis. Preparation, preparing all test apparatus that will be used as both supporting components and measurements, including meters, Flow Watch, Hand Tachometers, Ammeters, and Voltmeters.

At this stage, obtained after testing and data collection, the parameters measured are the rotation of the wheel, the rotation of the generator, the quantity of discharge, and the water flow speed. After all the tests have been completed, the performance data of the waterwheel can be obtained and further analysis can be conducted by creating a graph of the tested wheel's performance characteristics.

2.2 Methods

During the production of this waterwheel, a design has been chosen that has been adapted to the data acquired from field survey measurements in order to obtain the characteristics of the waterwheel that will be produced. The waterwheel's design criteria include its durability, uniform size and shape, and resistance to corrosion. Based on these criteria, the iron plate material was selected for the 2 mm waterwheel cover, and the used drum material was selected for the 1.5 mm waterwheel blade because it met the criteria in comparison to other materials. The

diameter of the waterwheel is 1100 mm, and its twelve blades are 700 mm wide.

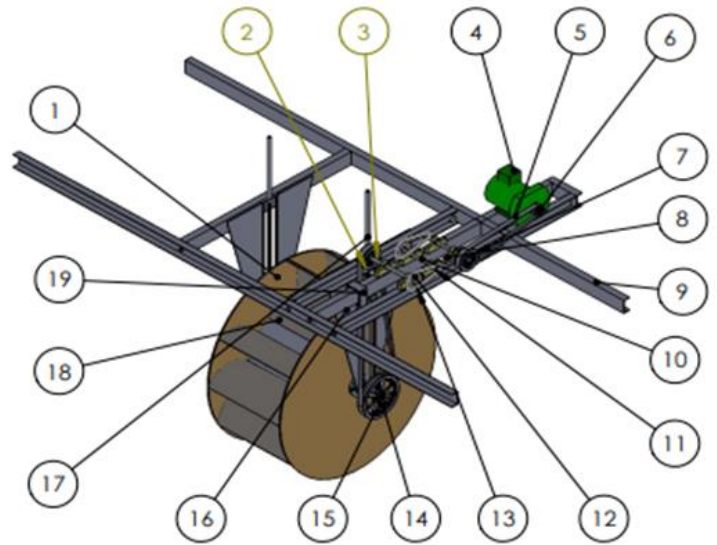
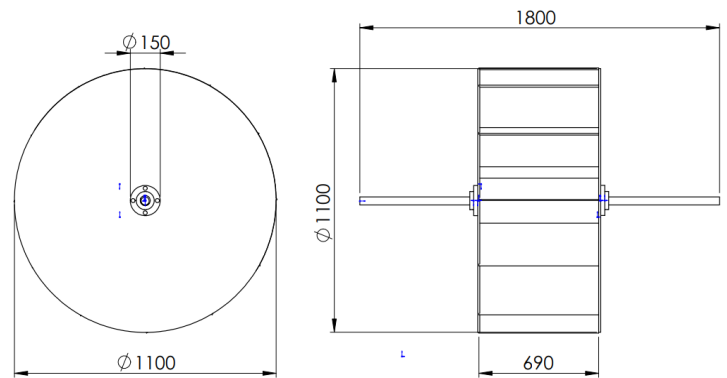


Fig. 1. Design of undershot waterwheel with chain transmission mechanism to drive an electric generator

Fig. 1 shows the names of undershot waterwheel components: (1) Blade holder plate with a thickness of 2 mm for holding the waterwheel blade; (2) Fan belt B115 type for waterwheel rotation transmission; (3) Pulley 6 inches for transmitting the mechanical power of the waterwheel to the gear transmission mechanism; (4) Generator of the asynchronous type for generating electrical energy; (5) Fan belt B77 type for transmitting power from the gear transmission mechanism to the generator. (6) Pulley of three inches for mechanical power transmission from the gear to the generator pulley; (7) Pulley of eight inches for mechanical power transmission. (8) Pillow block measuring three-quarters of an inch; (9) UNP 100 mm x 50 mm x 5 mm as a waterwheel support frame; (10) Shaft 20 mm in the gear transmission; (11) Sprockets Z16 type to support transmission using chains; (12) Gear to transmit mechanical power to an electric generator; (13) Sprockets Z40 type to support transmission using chains; (14) Pulley 16 inches to transmit mechanical power from the waterwheel to the gear mechanism; (15) Shaft 50 mm for transmitting mechanical power through the pulley; (16) Arm with a length of 1100 mm to hold the waterwheel atop.

The results of the undershot waterwheel test are shown in Table 1, along with the test parameters electrical loading, wheel rotation, generator rotation, electric current, voltage, water flow rate, and water velocity.

Table 1. Test results data on the undershot waterwheel

Electric Load (W)	Waterwheel Rotation (RPM)	Generator/ Electric Power (RPM)	Electric Current (A)	Voltage (V)	Mass flow rate ($\frac{m^3}{s}$)	Water Velocity ($\frac{m}{s}$)
0	48,42	2152	0	345	0,476	3,229
100	45	2000	0,6	293	0,476	3,229
140	42.39	1884	0,75	276	0,476	3,229
180	31.185	1386	0,8	203	0,476	3,229
200	30.082	1337	0,85	194	0,476	3,229
240	27.697	1231	0,95	160	0,476	3,229
280	25.402	1129	1	148	0,476	3,229
300	24.885	1106	1,05	136	0,476	3,229
340	23.872	1061	1,1	110	0,476	3,229
380	23.152	1029	1,2	100	0,476	3,229
400	22.425	996.7	1,25	92	0,476	3,229
440	21.307	947	1,3	90	0,476	3,229
480	20.661	918,3	1,35	84	0,476	3,229
500	20.571	914,3	1,4	80	0,476	3,229
540	19.836	881,6	1,45	74	0,476	3,229
580	19.192	853	1,5	70	0,476	3,229
600	18.99	844	1,5	68	0,476	3,229
640	18.184	808,2	1,55	64	0,476	3,229
680	17.172	763,2	1,55	60	0,476	3,229
700	16.989	755,1	1,6	55	0,476	3,229
740	16.254	722,4	1,6	50	0,476	3,229
780	15.592	693	1,65	45	0,476	3,229
800	15.255	678	1,7	42	0,476	3,229

3 Results and Discussion

The test results were obtained by following the research procedure, which included measuring the water head at the sluice with a ruler, measuring the speed of water flow with a flow watch, constructing a series of ammeters, voltmeters, and generators with spade and crocodile cables, lowering the wheel to its maximum position, and turning it on. generator, starting the test with a load of 0 W, measuring the speed of rotation on the generator shaft with a hand tachometer, reading the current flowing with an ampere meter at each loading, reading the voltage at the generator output with a voltmeter at each loading, recording the results of the generator current, generator voltage, and the rotational speed of the generator shaft, cleaning up the equipment after the test, processing the data, and recording the rpm of the generator.

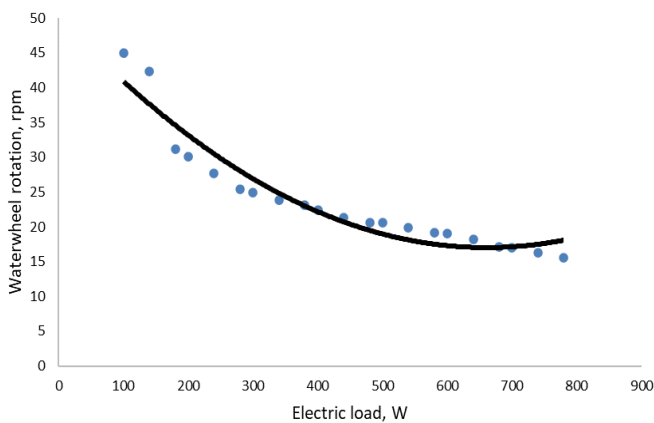


Fig. 2. Characteristics of turbine rotation toward the electric load
 Fig. 2 shows that the higher the installed lamp load, the lower the rotation of the waterwheel produced. In addition, it can be seen

that at a lamp load of 100 W, the rotation of the wheel can reach 45 rpm. The rotation speed of the waterwheel decreases to 15.255 rpm along with the increase in the highest lamp load at the time of testing, which is 800 W.

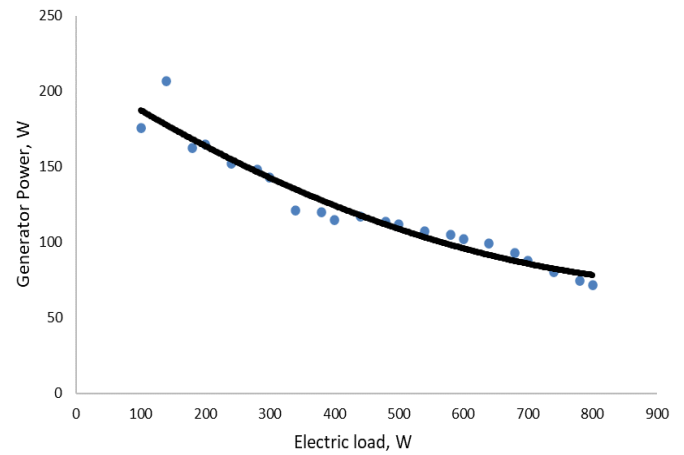


Fig. 3. Characteristics of generator power toward the electric load

Fig. 3 explained that the highest electrical power that can be achieved is 207 W at a lamp load of 140 W, and the discharge tends to be constant. While the highest lamp load that can be achieved is 800 watts, with a voltage of 42 V and the lowest power achieved is 71.4 W. The above is influenced by the rotation of the pinwheel which decreases with increasing electrical load. So that as the lamp load increases, lower electrical power is generated. From the data above, the maximum power occurs at a voltage of 276 V, because at that point, a current of 0.75 A is generated. So that the optimal power is 207 W.

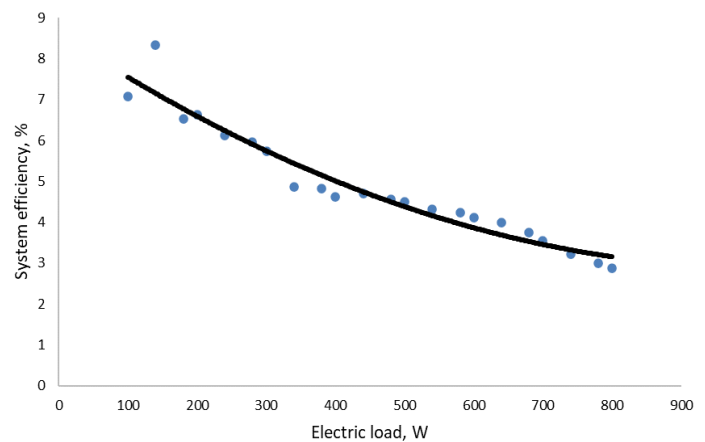


Fig. 4. Characteristics of system efficiency toward the electric load

Efficiency is generated by calculating electrical power divided by hydraulic power. Electrical power is influenced by the voltage and current generated by the generator. The higher the electrical power generated in the installation of certain lamp loads, the higher the efficiency that can be achieved. Fig. 4 shows that the highest efficiency of about 8.35% is obtained at the installation of a 140 W lamp load. While the lowest efficiency of about 2.88% is obtained at the installation of the highest lamp load of 800 W.

4 Conclusions

The following are the turbine's specifications: The diameter of the turbine is 1.1 meters, the width of the turbine is 0.7 meters, the flow rate is 0.476 m³/s, the water level at the water channel is 0.64 meters, the rotational speed of the turbine is 42.39 revolutions per

minute, the electric power is 207 watts, the voltage is 276 volts, and the capacity is 140 watts. The investigation of a micro-hydroelectric power facility with a waterwheel drive led to the following findings: The maximum wheel rotation at 100 W electrical load is 45 rpm, while the minimum wheel rotation at 800 W electrical load is 15.255 rpm. The highest achievable electrical power is 207 watts at a lamp load of 140 watts, while the lowest achievable electrical power is 71.4 watts at an 800-watt lamp load; the highest efficiency is 8.35% at a lamp load of 140 watts, while the lowest efficiency is 2.88% at an 800-watt lamp load. The waterwheel's characteristics produce the highest system efficiency of 8.35% at 42.39 rpm, which generates 207 Watts of electrical power, and the lowest efficiency of 2.88% at 15.255 rpm generates 71.4 Watts of electrical power.

Acknowledgments

The authors gladly recognize research financial support provided by Penelitian Terapan Unggulan Program Studi scheme P3M Politeknik Negeri Semarang, the Indonesian Ministry of Education, Culture, Research, and Technology in 2023.

References

- [1] Y.D. Herlambang, S.C. Lee, & H.C. Hsu, "Numerical estimation of photovoltaic-electrolyzer system performance on the basis of a weather database." *International Journal of Green Energy*, vol. 14, no.7, pp. 575-586, 2017.
- [2] Y.D. Herlambang, A. Roihadin, S.C. Lee, & J.C. Shyu, "MEMS-Based Microfluidic Fuel Cell for In Situ Analysis of the Cell Performance on The Electrode Surface." *Journal of Physics: Conference Series*, IOP Publishing, vol. 1444, no. 1, pp. -12044, 2020.
- [3] Y.D. Herlambang, S.C. Lee, J.C. Shyu, & C.J. Liu, "Numerical study and modeling of the solar radiation measurement on tilted surface for the local behavior database," *Journal of the Chinese Society of Mechanical Engineers*, vol. 37, no.5, pp. 441-448, 2016.
- [4] Y.D. Herlambang, & S.C. Lee, "Application of Electrochemical Supercapacitor to Photovoltaic System on Unmanned Flying Machine," *Smart Grid Renew. Energy*, vol. 5, no. 4, pp. 77-87, 2014.
- [5] Y.D. Herlambang, Supriyo, B. Prasetyo, A.S. Alfauzi, T. Prasetyo, Marliyati, and F. Arifin, "Experimental and Simulation Investigation on Savonius Turbine- Influence of Inlet-Outlet Ratio Using a Modified Blade Shaped to Improve Performance," *Evergreen-Joint Journal of Novel Carbon Resource Sciences & Green Asia Strategy*, vol. 9, no. 2, pp. 457-464, 2022.
- [6] D. Adanta, S.A. Arifianto, S.B. Nasution, & Budiarto, "Effect of blade number on undershot waterwheel performance with variable inlet velocity," *4th International Conference on Science and Technology (ICST)*, Yogyakarta, Indonesia, 2018.
- [7] E. Quaranta, & G. Muller, "Optimization of undershot water wheels in very low and variable flow rate applications. *J. Hydraul. Res.*, pp. 845-849, 2019.
- [8] I.L.K. Wong, A. Buku, J.E. Latupeirissa, & H.C.P. Tiwouy, "Performance of undershot waterwheel curved blade of the laboratory scale," *Mater. Sci. Forum*, vol. 967, pp. 250-255, 2019.
- [9] F.M. White. *Fluid Mechanics*. 5th edition, McGraw-Hill, University of Rhode Island, USA, 2016.
- [10] D.P. Sari, Helmizar, I. Syofii, Darlius, & D. Adanta, "The effect of the ratio of wheel tangential velocity and upstream water velocity on the performance of undershot waterwheels," *J. Adv. Res. Fluid Mech. Therm.Sci.*, vol. 65, no. 2, pp. 170-177, 2020.
- [11] W. Warjito, D. Adanta, B. Budiarto, S.B.S. Nasution, & M.A.F. Kurnianto, "The Effect of Blade Height and Inlet Height in a Straight-Blade Undershot Waterwheel Turbine by Computational Method," *CFD Lett.*, vol. 11, no. 12, pp. 66-73, 2020.
- [12] I.L.K. Wong, J.E. Latupeirissa, & H.C.P. Tiwouy, "A Laboratory Scale Curve Bladed Undershot Water Wheel Characteristic as an Irrigation Power," *Int. J. Mech. Eng.*, vol. 9, no. 9, pp. 1048-1054, 2018.
- [13] E.Y. Setyawan, S. Djiwo, D.H. Praswanto, P. Suwandono, & P. Siagian, "Design of low flow undershot type water turbine," *J. Appl. Sci. Eng.*, vol. 2, no. 2, pp. 50-55, 2019.
- [14] Y. Kikuchi, T. Kiwata, S. Watada, & T. Kono, "Experimental study on performance of undershot water wheel in snow drainageway at shiramine district by field test," *Adv. Exp. Mech.*, vol. 3, pp. 104-110, 2018.
- [15] C. Promdee, & C. Photong, "Sustainability assessment of hydropower water wheels with downstream migrating fish and blade strike modelling," *Sustain. Energy Technol. Assess.*, vol. 43, pp. 100943, 2016.
- [16] L. Syofii, D.P. Sari, D. Adanta, M.A.A. Saputra, & Wadirin, "Moving Mesh as Transient Approach for Pico Scale Undershot Waterwheel," *CFD Lett.*, vol. 14, no. 8, pp. 33-42, 2022.
- [17] G. Todorov, K. Kamberov, & M. Semkov, "Improvement of undershot water wheel performance through virtual prototyping," *Appl. Math. Eng. and Econ.*, vol. 2333, pp. 110011-1-110011-7, 2021.
- [18] A. Buku, & B. Tangaran, "Planning of Flat Plate Undershot Waterwheel as Mini Hydro Power Plant and Irrigation Power in Remote Areas," *Int. J. Adv. Eng. Tech.*, vol. 11, no. 12, no. 342-349, 2020.
- [19] M. Darmawi, I. Bizzy, & R. Sipahutar, R., "Undershot Floating Waterwheel a Concept of Small Hydropower Energy Development for Rural Areas of Indonesia," *J. Mech. Eng. Res. Dev.*, vol. 45, no. 2, pp. 3-9, 2022.
- [20] J.A. Hameed, A.T. Saeed, & M.H. Rajab, "Design and Study of Hydroelectric Power Plant by Using Overshot and Undershot Waterwheels," *International Journal of Energy Optimization and Engineering*, vol. 8, no. 4, pp. 39-58, 2019.
- [21] Y.D. Herlambang, K. Kurnianingsih, A. Roihadin, F. Arifin, "Model experimental of photovoltaic-electrolyzer fuel cells as a small-scale power. International Conference on Vocational Education of Mechanical and Automotive Technology. IOP Publishing, Yogyakarta Indonesia, 5 Oktober 2020, *Journal of Physics: Conference Series*, vol. 1700, no. 1, pp. 012100, 2020.
- [22] Y.D. Herlambang, T. Prasetyo, A. Roihadin, Y.M. Safarudin, & F. Arifin, "Hybrid Power Plat of the Photovoltaic-Fuel Cell," *IOP Conf. Series: Materials Science and Engineering*, International Conference on Innovation in Science and Technology (ICIST 2019), IOP Publishing, vol. 1108, pp. 012049, 2021.
- [23] E. Antar, & M. Elkhoury, "Parametric sizing optimization process of a casing for a Savonius vertical axis wind turbine," *Renew. Energy.*, vol. 136, pp. 127-138, 2019.
- [24] A.L. Manganhar, A.H. Rajpar, M.R. Luhur, S.R. Samo, & M. Manganhar, "Performance analysis of a Savonius vertical axis wind turbine integrated with wind accelerating and guiding rotor house," *Renew. Energy.*, vol. 136, pp. 512-520, 2019.
- [25] A.S. Saad, L.L. Sharkawy, S. Ookawara, & M. Ahmed, "Performance enhancement of twisted-bladed Savonius vertical axis wind turbines," *Energy Convers. Manag.*, vol. 209, no. 112673, pp. 1-19, 2020.

- [26] R. Alipour, R. Alipour, F. Fardian, S.S.R. Koloor, & M. Petru, "Performance improvement of a new proposed Savonius hydrokinetic turbine: a numerical investigation," *Energy Rep.*, vol. 6, pp. 3051-3066, 2020.
- [27] M.E. Nimvari, H. Fatahian, & E. Fatahian, "Performance improvement of a Savonius vertical axis wind turbine using a porous deflector," *Energy Convers. Manag.*, vol. 220, no. 113062, pp. 1-13, 2020.
- [28] S. Sharma, & R.K. Sharma, "Performance improvement of a Savonius rotor using multiple quarter blades-A CFD investigation," *Energy Convers. Manag.*, vol. 127, pp. 43-54, 2016.
- [29] M. Zemamou, M. Aggour, & A. Toumi, "Review of Savonius wind turbine design and performance," *Energy Procedia.*, vol. 141, pp. 383-388, 2017.
- [30] H. Belmili, R. Cheikh, T. Smail, N. Seddaoui, & R.W. Biara, "Study, design, and manufacturing of hybrid vertical axis Savonius wind turbine for urban architecture," *Energy Procedia.*, vol. 136, pp. 330-335, 2017.
- [31] S.C. Goh, S.R. Boopathy, C. Krishnaswami, & J.U. Schluter, "Tow testing of Savonius wind turbine above a bluff body complemented by CFD simulation," *Renew. Energy.*, vol. 87, pp. 332-345, 2016.